

Highlight of a Compensation Effect Between Filler Morphology and Loading on Dynamic Properties of Filled Rubbers

Franck Sosson, Lénaïk Belec, Jean-François Chailan, Pascal Carriere, Alain Crespy

Laboratoire Matériaux Polymères Interfaces Environnement Marin (MAPIEM) EA 4323, Université du Sud-Toulon-Var, BP 20132, 83957 La Garde Cedex, France

Received 16 March 2009; accepted 27 July 2009

DOI 10.1002/app.31216

Published online 27 April 2010 in Wiley InterScience (www.interscience.wiley.com).

ABSTRACT: This investigation highlighted the equivalence between carbon black (CB) loading and structure influences on dynamic mechanical properties in the linear behavior of several filled synthetic rubber compounds. Different morphologies (specific surface area and structure) of CB incorporated at different loadings were formulated to modulate the filler-rubber matrix interphase content, usually named “tightly bound rubber.” Both reinforcement level and tightly bound rubber content were measured on each compound by dynamic mechanical analysis (DMTA) and by Soxhlet extraction and thermogravimetry (TGA) respectively. Then, a systematic description of their evolution was made against CB loading and

morphology. These evolutions were attributed to the hydrodynamic effect which could be evaluated by the effective filler volume fraction. A new parameter κ is defined, representing the effective filler volume fraction for each compound and it was calculated on the basis of experimental parameters. Results show good correspondences between κ included both the hydrodynamic effects of the filled carbon black rubbers and dynamic mechanical properties. © 2010 Wiley Periodicals, Inc. *J Appl Polym Sci* 117: 2715–2723, 2010

Key words: elastomers; interfaces; reinforcement; structure-property relations; viscoelastic properties

INTRODUCTION

Different kinds of fillers, especially carbon blacks (CB), are present in vulcanized rubber matrix to enhance such properties as strength, stiffness, and tear or abrasion resistance. The applications of filled rubbers are numerous and require a high level of understanding of their mechanical properties. They include automotive engine mounts, vibration and sonic isolation systems, and impervious systems. The prediction of the performance and the mechanical evolutions of such devices is then very important.

Most theories describe the effect of fillers on the rubbers reinforcement by the hydrodynamic effect. Guth and Gold have developed a basic theory of this model to describe rubber reinforcement¹ and its effect on dynamic mechanical properties. They obtained the evolution of the storage modulus as follows:

$$G' = G'_0 \left(1 + 0.67f \cdot \phi + 1.62f^2 \phi^2 \right) \quad (1)$$

where G' and G'_0 are storage moduli of filled and vulcanized gum, respectively, ϕ the volume fraction

of the filler and f a shape factor, which describes the asymmetric particle as expressed by the ratio of their length to their diameter.

This equation is still valid with concentration up to a few percent (less than 30 %) only. However, filler structure, characterized by DBPA, was found to have a dominant influence on f .² The deviation becomes more significant when both the volume loading and the structure (higher DBPA) of CB are high.^{3,4} One approach to correct this deviation is to consider that the effective filler volume loading is larger than the one calculated from the weight loading of carbon. This is the concept of rubber occluded within the internal void space of the primary structure filler aggregates. This occluded rubber is partly shielded from deformation, and thus acts as part of the filler rather than as part of the matrix. In fact, the amount of rubber bearing the stresses imposed to the sample is reduced by the amount of occluded rubber. The effective filler volume fraction is the sum of the CB volume fraction plus the occluded rubber (called ϕ'). It can be calculated from the volume fraction alone ϕ and a direct measure of the internal CB volume (DBPA):

$$\frac{\phi'}{\phi} = \frac{46.75 + \text{DBPA}}{68.26} \quad (2)$$

However, the DBPA test does not predict the real internal CB volume, which is broken during

Correspondence to: L. Belec (belec@univ-tln.fr).

Contract grant sponsor: Provence-Alpes-Côtes d'Azur.

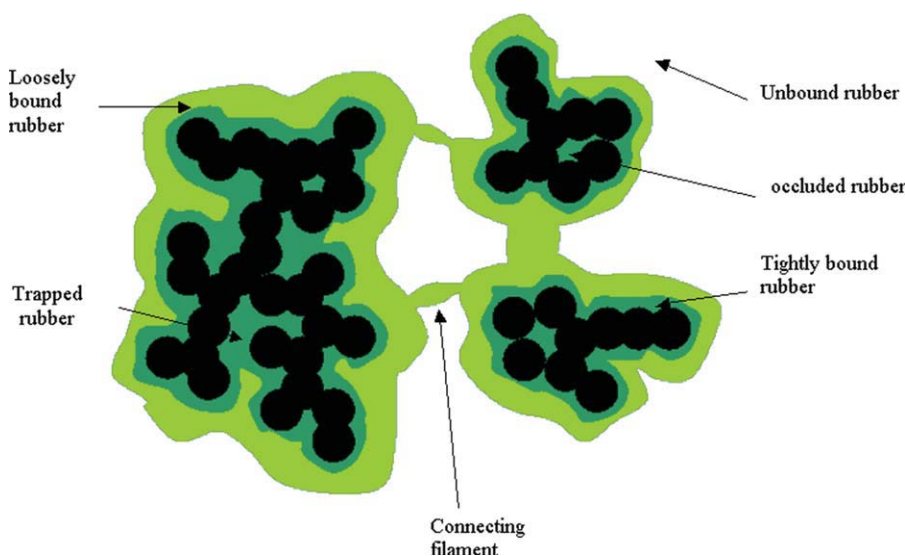


Figure 1 Pictorial description of the morphology of carbon-black filled rubber compounds.¹⁶ [Color figure can be viewed in the online issue, which is available at www.interscience.wiley.com.]

incorporation in rubber. The void ratio within the aggregates is somewhat lower after fracture, as shown by the crushed DBPA (cDBPA) test in which the CB is crushed four times before measuring the DBPA.^{4,5} Then the effective volume fraction ϕ' can be calculated as follows:

$$\frac{\phi'}{\phi} = \frac{24 + \text{cDBPA}}{55} \quad (3)$$

The occluded rubber can be determined by specific extraction techniques from uncured filled polymer compounds.⁶⁻⁹ Above a filler content threshold, a gel containing both bound rubber and filler particles can be detected. The respective fractions of occluded rubber and filler can thus be determined through thermo gravimetric measurements. Moreover, the occluded rubber has been highlighted by nuclear magnetic resonance (NMR).¹⁰⁻¹² The unbound polymer was first extracted at room temperature by an appropriate solvent during a sufficient time,^{8,13} and the bound rubber (loosely and tightly bound rubber, Fig.1)¹⁴ was next dried in vacuum and analyzed. Recently, Kaufmann et al.¹⁵ and other authors¹⁶ show that the segmental motions of the rubber molecules in the occluded rubber are constrained in comparison to the molecular motions in the pure rubber. The bound rubber is composed of an immobilized region immediately surrounding the CB and a region of intermediate mobility. In the later, the polymer segmental motions are free from physical interactions with the CB surface in comparison to the immobilized region, but constrained in comparison to the motions in the pure (bulk) rubber. So, each analysis methods are agreed to demonstrate that bound rubber forms an onion like structure as previously presented.¹⁷

In parallel, numerous works have reported the equivalence between the influence of both CB loading and CB structure on mechanical properties and bound rubber content.^{5,18} However, Medalia¹⁹ reviewed several studies on different CB grades at various loadings in SBR. He linked $\tan \delta$ values (measured at 60°C, 14.5% static compression, 20% Dynamic Strain Amplitude, 0.25 Hz) for each compound to a simple combined function of specific surface area ψ and loading ϕ , $\phi\psi$, called loading-interfacial area parameter. With $\psi = \rho S\phi$ it gives:

$$\phi\psi = \rho S\phi^2 \quad (4)$$

where ρ is the density of CB generally taken as 1.80 to 1.86 g cm⁻³, and S is the CTAB area (Cetyl Trimethylammonium Bromide method). A linear relation was found using $\tan \delta$ calculated from pendulum rebound on several rubber types, but in all cases extrapolation of $\tan \delta$ to zero $\phi\psi$ gave a higher value than the pure gum one. Recently, Choi²⁰ distinguished macromolecules as loosely and tightly bound to the CB and shows an increase of the Mooney viscosity and Mooney peak with CB structure. Those evolutions were related to the increase of the bound polymers according to the CB morphology.

Moreover, the effect of fillers contents and nature on shear modulus is often explained by the development of a percolating network by the filler particles. Different models take account of the effective volume fraction of reinforcing phase via filler-filler or filler polymer interactions²¹⁻²³ and cluster aggregation phenomena.²⁴ Under dynamic mechanical solicitations in linear viscoelastic range, increasing filler volume fraction increases the elastic modulus, especially in rubber state, and decreases the amplitude

TABLE I
Physical Characteristics of Carbon Black

Ref.	Cabot ref.	STSA Specific surface area (m ² g ⁻¹)	Iodine adsorption (mg g ⁻¹)	Crushed DBP (mL 100 g ⁻¹)	DBP (mL 100 g ⁻¹)
A	N772	31	30	58	65
B	N550	50	43	84	121
C	N347	82	90	96	124

as well as the temperature at $\tan \delta$ maximum.²⁵ The evolution of G' can be explained by the global increase of the reinforcement phase (filler and bound rubber) or by the cluster aggregation model. Indeed, according to that theory, the storage modulus of the filler network is proportional to $V^{3.5}$, V being the filler volume fraction. The modulus resulting from both phases should then increase with V .

The influence of the filler contents on the temperature of the main relaxation has been attributed by Mele et al.²⁵ to a particular mechanical coupling effect between the three phases model: particles, bound rubber, and unmodified rubber.

In spite of the numerous theories cited earlier, based on many experimental studies, none of them can fully explain dynamic mechanical properties of rubber-filled compounds on the linear behavior. In this article, we focus on the influence of reinforcement on the linear viscoelastic behavior.

We show the combined influence of CB loading and morphology on dynamic mechanical properties of such rubber compounds. Combinations of both parameters lead to different levels of reinforcement and allow us to define a new parameter, named κ , which takes into account the equivalence between CB loading and structure involved in the effective filler volume fraction.

EXPERIMENTAL SECTION

Test procedure

The dynamic mechanical properties of various samples were characterized by dynamic mechanical thermal analyzer (DMA 2980 from TA Instruments), with the single cantilever mode on a rectangular sample of 3–4 mm thickness, 17.5 mm length, and 15 mm width. Temperature sweeps measurements were carried out between -100°C and $+20^{\circ}\text{C}$ at 1 Hz with a programmed heating rate of $1^{\circ}\text{C min}^{-1}$ using liquid nitrogen cooling accessory. The strain amplitude was set at 0.04% in order to stay in the linear viscoelastic range of each sample. The parameters studied in this work are, the storage modulus G' and its value at 20°C ($G'_{20^{\circ}\text{C}}$), the maximum $\tan \delta$ measured at the top of the peak, and $\tan \delta$ peak area which is measured by TA Universal Analysis between -90°C et 20°C . In those experiments shearing doesn't exceed 0.1%, the dynamic

mechanical testing devices produce nearly perfectly sinusoidal reference signal, without any harmonics.

The CB weight content was verified by Thermogravimetry Analysis (TGA Q600 from TA Instruments) according to NF T46-047 standard. It consists of heating at $20^{\circ}\text{C min}^{-1}$ under nitrogen upto 600°C , cooling down to 400°C , and heating under air at $20^{\circ}\text{C min}^{-1}$ upto 850°C . The weight fraction of CB and inorganic residue can then be determined.

The extraction using boiling toluene (bp, 110°C) were carried out in a 200 mL Soxhlet extractor.^{8,13,26} Approximately 1 g of each unvulcanized rubber compound cut into small pieces was introduced in the Soxhlet basket. After one week without changing the solvent, the basket containing the swollen sample (coherent gel) was dried at 60°C for 48 h under vacuum. Then the gel containing both tightly bound rubber,¹⁹ CB, and insoluble ingredients were pyrolysed with TGA under air (100 mL min^{-1} , $10^{\circ}\text{C min}^{-1}$). All experiments were carried out three times.

Materials

The rubber used in this study is a butyl rubber. Different CB reinforcing fillers were chosen for their different structures and specific surface areas Table I. The CB references N772, N550, and N347 according to Cabot are respectively designated as A, B and C for readability (Table I). The structure is the staking mode of the CB primary particle. It can be evaluated by the measure of the empty space (void volume) in aggregates, usually expressed as the volume of dibutylphthalate (DBP) absorbed by a given amount of CB. During the cDBPA test, agglomerates are broken into aggregates and the DBP test is applied. High structure carbon blacks exhibit a high DBP or cDBP number and inversely. The specific surface area (or primary particle size) is the specific surface of a CB primary particle, which composes the aggregate. It is characterized by different adsorption methods of specified molecules: the iodine number and the Statistical Thickness Surface Area (STSA), which is an alternative technique for the determination of the external surface area. High specific surface areas give both high iodine adsorption and STSA numbers, and inversely.

Both specific surface area and structure modulate the potential surface area between fillers and rubber matrix, which increases between A and C.

TABLE II
Composition in 100 Parts by Weight of Rubber

Compound		N-0	A-35	A-65	A-100	B-65	C-65	C-77	C-100
Rubber		100	100	100	100	100	100	100	100
Carbon black	A	–	35	65	100	–	–	–	–
	B	–	–	–	–	65	–	–	–
	C	–	–	–	–	–	65	77	100
Process oil		5	7	13	20	13	13	15.4	20
Vulcanising agents		5.5	5.5	5.5	5.5	5.5	5.5	5.5	5.5

Samples preparation

Designations and compositions of samples used in this study are given in the Table II. In each blend, fillers and various additives were first dispersed into the polymer using a Banbury blender and secondly mixed in a two roll mixing mill to incorporate the vulcanization system. Mixing conditions have been optimized to obtain a good dispersion of CB in each compound. Cure properties of blends were determined by a rheometer (RPA 2000 from Alpha Technologies) at 160°C, 100 cpm). A 15 min sulphur cure at 160°C was applied to all the samples in a hydraulic hot-press to obtain crosslinked plates (3–4 mm in thickness). Before the measurements, all the samples were conditioned at room temperature for 24 h.

The sample named N-0 contains no CB to have dynamic mechanical properties reference of unload compound. The process oil loading is selected to have the same CB/process oil ratio in each sample. The amount of vulcanizing agents is fixed at 5.5 phr to keep a constant ratio between rubber and additives. Consequently, these agents should have the same influence on each compound.

Table III gives the corresponding weight fraction and volume fraction of CB measured by TGA for each compound. Results show that CB weight fractions are higher than those introduced in compounds during processing due to residual CB content in each mixer. This is well observed in the N-0 compounds where there is a few CB volume percent ($\approx 6\%$).

RESULTS AND DISCUSSION

Determination of tightly bound rubber content

For compound N-0, we suggest that the tightly bound rubber content and its participation to hydro-

dynamic effect are negligible in regard to the weak filler content (≈ 0.04). For the compound A-35, no coherent gel is obtained during Soxhlet extraction. The extraction of a weak part of the compound takes place and the tightly bound rubber content could not be measured.

A representative thermogravimetry spectrum, performed here on B65, is shown in Figure 2. Typically, two weight losses were observed during temperature sweep, identified as tightly bound rubber degradation below 400°C and CB degradation around 600°C.

Tightly bound rubber content was calculated considering that, before extraction, the sum of the weight fraction of each ingredient is equal to 1. Then:

$$X_{CB} + X_{oil} + X_{additives} + X_{extracted_rubber} + X_{tightly_bound_rubber} = 1 \quad (5)$$

After the extraction, if we assume that all the oil has been extracted but not the additives, the sum of the remaining ingredients in the basket is equal to 1:

$$Y_{CB} + Y_{additives} + Y_{tightly_bound_rubber} = 1 \quad (6)$$

Y_{CB} corresponds to the second weight loss in the thermogram (around 600°C), $Y_{tightly_bound_rubber}$ to the first weight loss (around 400°C), and $Y_{additives}$ is the residual sample weight above 600°C.

As no CB was extracted, we assume that:

$$\frac{Y_{CB}}{Y_{tightly_bound_rubber}} = \frac{X_{CB}}{X_{tightly_bound_rubber}} \quad (7)$$

Therefore, the tightly bound rubber weight content ($X_{tightly_bound_rubber}$) and its volume fraction can be calculated.

TABLE III
Phr Content, Actual Weight Fraction, and Actual Volume Fraction of Carbon Black for Each Compound

Compound	N-0	A-35	A-65	A-100	B-65	C-65	C-77	C-100
Theoretical carbon black weight fraction	0.00	0.24	0.37	0.44	0.37	0.37	0.39	0.44
Actual carbon black weight fraction	0.06	0.27	0.37	0.46	0.38	0.38	0.41	0.46
Actual carbon black volume fraction	0.04	0.17	0.24	0.31	0.24	0.24	0.27	0.31

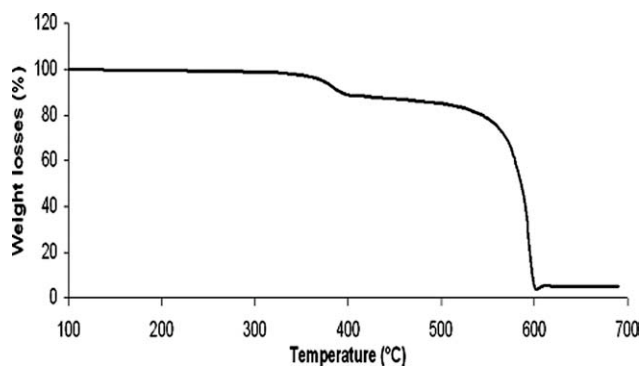


Figure 2 Typical thermogravimetry spectrum (10°C/min, air).

$$X_{\text{tightly_bound_rubber}} = X_{\text{CB}} \cdot \frac{Y_{\text{tightly_bound_rubber}}}{Y_{\text{CB}}} \quad (8)$$

Results are described in the Table IV. For CB grade A and C, tightly bound rubber volume fraction increases with CB content. This effect is more pronounced for CB C. Results have already been observed in literature^{7,9,27} and could be governed by different phenomena: (a) formation of tightly bound rubber adsorbed around filler, (b) formation of occluded rubber inside aggregates, and (c) formation of trapped rubber between aggregates. Results give also a tightly bound rubber volume fraction evolution more pronounced for CB C when CB content increases. Moreover, tightly bound rubber volume fraction increases with CB physical parameter, i.e., when both structure and specific surface area increase. Those evolutions will be treated and discussed thereafter.

Dynamic mechanical behavior of compounds

Figure 3 shows the storage modulus G' for vulcanized described in the Sample Preparation Section and Table II. It appears that in the glassy region (below -70°C for this particular polymer), a weak difference was observed between compounds, while in the rubbery region (above -20°C) modulus plateau level increases with both CB volume fraction and CB morphology (both specific surface area and structure increase).

The increase of G' level in the rubbery region (referred as $G'_{20^{\circ}\text{C}}$ further) is associated to an increase of both CB volume fraction and tightly

bound rubber volume fraction (Table IV). Since compounds are sollicitated in the linear viscoelastic range, the tightly bound rubber is not deformed and can then be assimilated as filler. In other words, the increase of the storage modulus with CB loading and morphology in the rubbery region is attributed to the increase of the hydrodynamic effect. This later can be measured by the effective filler volume fraction calculated from the sum of the CB volume fraction and the tightly bound rubber volume fraction. Results are described in the Table IV. The influence of the hydrodynamic effect is also observed on $\tan \delta$ spectra in the same experimental conditions (Table IV). Results show a decrease of both maximum $\tan \delta$ and $\tan \delta$ peak area when CB loading and/or CB morphology (both effective surface area and structure) increase. This may be interpreted in terms of a reduction in free polymer fraction (i.d. extractable rubber) in the compound, as the polymer would be responsible for the high portion of energy dissipation, and in parallel to an increase of the effective filler volume fraction, which does not dissipate energy significantly.

We can also observe that the temperature at maximum $\tan \delta$ decreases with both CB loading and CB morphology. This shows an increase of the elastomer segments mobility participating to the relaxation, i.e. decreasing average relaxation time. This evolution could be attributed to the preferential rubber-filler interaction of the largest molecular weight fractions.²⁸ As the filler-rubber interaction surface increases with both CB loading and CB morphology, the participation of the largest molecular weight to the matrix relaxation disappears and the temperature at the maximum $\tan \delta$ decreases.

Evolutions of G' in the rubbery region, maximum $\tan \delta$ and $\tan \delta$ peak area are associated to various microstructure modifications, which increase the content of a rigid phase in compounds. Hydrodynamic interactions increase with the CB content resulting from an adsorption process of the rubber matrix chains on the filler surface, and in the void spaces of the aggregate (i.d. occluded rubber). This adsorption process originates from the existence of weak links between filler particles and segments of rubber chains.²⁹ This process leads to the formation of an hard rubber shell surrounding the filler, due to the low mobility of polymer chains adsorbed on the filler surface.^{17,22,30} So, when the CB loading increases, both occluded rubber and rubber/filler

TABLE IV
Tightly Bound Rubber Content and the Effective Filler Volume Fraction

Compound	N-0	A-35	A-65	A-100	B-65	C-65	C-77	C-100
Tightly bound rubber volume fraction	0.00	–	0.08	0.07	0.09	0.18	0.22	0.26
Effective filler volume fraction	0.04	–	0.32	0.38	0.33	0.42	0.49	0.57

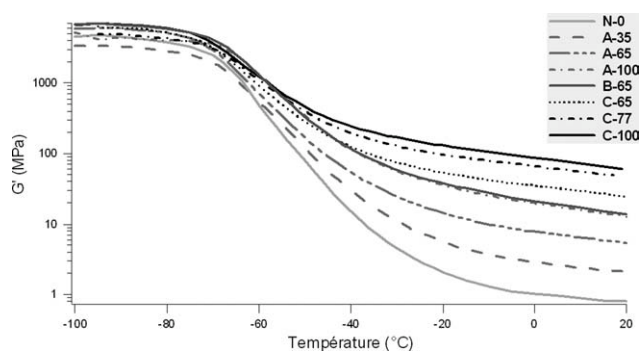


Figure 3 Dynamic mechanical spectra; temperature dependence of the storage modulus G' for all vulcanized rubber compounds (1 Hz, 0.04 %, 1°C/min).

links (hard rubber shell content) increase. The hydrodynamic effect is then increased by the introduction of a rigid phase composed with both CB and tightly bound rubber called effective volume fraction (Table IV). Moreover, the introduction of CB decreases inter-aggregate distances,^{22,30} and so immobilizes rubber chains between filler agglomerates by confinement effects. This is the concept of the trapped rubber.³¹ This process is more pronounced for the filler C as we will discuss later.

Similar evolution of the mechanical properties are observed when CB physical properties increase (specific surface area and structure) at constant CB loading: $G'_{20^\circ\text{C}}$ increases (Fig. 3) and both maximum $\tan \delta$ and $\tan \delta$ peak area decrease (Fig. 4). The influence of both CB specific surface area and structure has two main origins. On one hand, when CB specific surface area increases, the primary particle size decreases and so distances between aggregates and/or agglomerates decrease.^{22,30} Moreover, for good filler dispersion, the filler-rubber interface increases. When CB rate is above percolation threshold, it leads to an increase of the tightly bound rubber adsorbed around the filler and trapped between aggregates and/or agglomerates. On the other hand, when CB structure increases, the void space inside the filler increases and the occluded rubber content increases too.

Thus, concerning the CB structure, cDBPA test shows a larger difference between the references A and B than between the references B and C (Table V).

This is also observed on the dynamic mechanical properties (Table V), which show a more pronounced change between compounds A-65 and B-65 than between compounds B-65 and C-65. Moreover, iodine numbers, which measure the CB specific surface area, are close for CB A and B but the double between CB B and C.

To conclude, for our series of compounds, CB structure seems to be the preponderant parameter (rather than CB effective surface area) influencing dynamic mechanical properties. Its effect increases with the CB specific surface area because the trapped rubber content increases as the interparticle distance decreases.

Introduction of a new parameter for carbon black content/morphology compensation

Considering compounds A-100 and B-65 (Fig. 5), we observe that the storage modulus G' and $\tan \delta$ spectra are nearly superimposed. This suggests a compensation phenomenon between CB volume fraction and the CB structure on the hydrodynamic effect. High filler structure used at low concentration gives the same effects as lower structure filler used at high concentration. In fact, the carbon black B-65 is more structured than the carbon black A-100, which is in higher proportion. Table IV shows close effective filler volume fraction for those two compounds (respectively 0.38 for compound A-100 and 0.33 for compound B-65).

So, for CB (loadings and grades) investigated in this work, the accessible surface, and so the tightly bound rubber adsorbed, occluded and trapped increase with both CB loading (at constant CB structure) and CB structure (at constant CB loading). The total accessible surface could be estimated by a combination of both CB volume fraction and structure effect. Since the loading is above percolation threshold, we postulated, for CB content investigated in this work, that filler agglomerations are numerous and the cDBPA test is associated to a surface property and not to a volume property. With the use of a chemical absorption process of the DBP molecule on the CB filler, the number of DBP molecules absorbed on 1 g of filler is:

TABLE V
Dynamic Mechanical Properties for Compounds with 65 phr Carbon Black Content

Compound	Carbon black physical tests		Dynamic mechanical properties		
	Iodine number (mg g^{-1})	cDBPA ($\text{mL } 100\text{g}^{-1}$)	$G'_{20^\circ\text{C}}$ (MPa)	maximum $\tan \delta$	$\tan \delta$ peak surface area (a.u.)
A-65	30	58	5.4	1.0	36.5
B-65	43	84	12.8	0.8	27.0
C-65	90	96	24.4	0.7	22.4

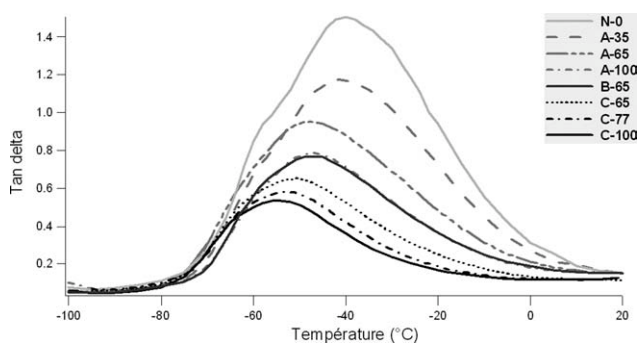


Figure 4 Dynamic mechanical spectra; temperature dependence of $\tan \delta$ for all vulcanized rubber compounds (1 Hz, 0.04 %, 1°C/min).

$$n_{\text{DBP}} = \frac{c_{\text{DBPA}}}{V_{\text{DBP}} \cdot 100} \quad (9)$$

where V_{DBP} is the volume of one DBP molecule that we have estimated at $20 \cdot 10^{-24}$ mL calculated with the use of the DBP geometric molecule and the distance between atoms. The interaction surface area S_i between the rubber matrix and 1 g of CB is then:

$$S_i = n_{\text{DBP}} \cdot s_{\text{DBP}} \quad (10)$$

where s_{DBP} is the DBP molecule surface in contact with the CB, estimated with the average diameter of a sphere which envelopes the DBP molecule. We have then defined a new parameter ' κ ' (kappa), similar to a specific surface area, which is the product of the CB volume fraction and the CB specific surface area derived from cDBPA parameter:

$$\kappa = \phi_{\text{CB}} \cdot S_i \quad (11)$$

where ϕ_{CB} is the CB volume fraction.

κ values for each compound are summarized in Table VI. In spite of the fact that the compound N-0 contains a weak CB volume fraction, we estimate its total specific surface area equal to zero.

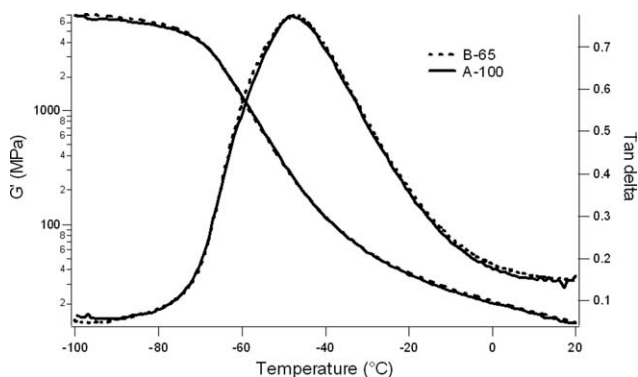


Figure 5 Dynamic mechanical spectra; temperature dependence of G' and $\tan \delta$ for compounds A-100 and B-65 (1 Hz, 0.04 %, 1°C/min).

TABLE VI
Total Specific Surface Area

Compound	Carbon black volume fraction	Specific surface area derived from cDBPA test (m^2/g)	Total specific surface area, κ (m^2/g)
N-0	0.04	0	0
A-35	0.17	99	17
A-65	0.24	99	23
A-100	0.31	99	31
B-65	0.24	143	35
C-65	0.24	163	40
C-77	0.27	163	44
C-100	0.31	163	49

The calculations for the total specific surface area, written κ , are significantly different for each compound. Moreover, compounds A-100 and B-65 have a close κ .

Results on dynamic mechanical properties show regular evolutions between κ and both $G'_{20^\circ\text{C}}$ (Fig. 6) and $\tan \delta$ peak area (Fig. 7). This confirms the compensation phenomenon between CB volume fraction and CB structure on dynamic mechanical properties. The increase of $G'_{20^\circ\text{C}}$ is related to the increase of the effective filler volume fraction, which can be assimilated to a "hydrodynamic effect."

Figure 8 shows a linear relation between κ and the effective filler volume fraction, which is an experimental parameter (Table IV). This linearity can be written as follows:

$$\kappa = \alpha \cdot \phi_v \quad (12)$$

where α is a ratio coefficient and ϕ_v the effective filler volume fraction.

With the definition of κ , eq. (13) becomes:

$$\phi_{\text{CB}} \cdot S_i = \alpha \cdot (\phi_{\text{CB}} + \phi_{\text{TBR}}) \quad (13)$$

where S_i is the total interaction surface area between the rubber matrix and fillers, ϕ_{CB} is the initial CB volume fraction, and ϕ_{TBR} is the volume fraction of the tightly bound rubber.

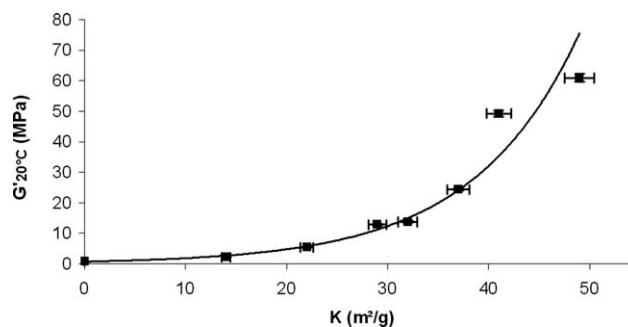


Figure 6 Influence of κ on the storage modulus measured at 20°C.

So, the ratio coefficient is:

$$\alpha = \frac{S_i}{1 + \frac{\phi_{\text{TBR}}}{\phi_{\text{CB}}}} \quad (14)$$

therefore, for a given CB, this equality is verified if the ratio $\phi_{\text{TBR}}/\phi_{\text{CB}}$ is constant.

Dependences of G' and $\tan \delta$ with both CB volume fraction and with specific surface area has often been pointed out separately. However, no proportional relationship has been clearly established between these parameters. Moreover, no compensation effect had been clearly shown.

The linearity between κ and ϕ_v involves that the volume fraction of the tightly bound rubber and the CB volume fraction are proportional, and yet, the tightly bound rubber takes account of occluded, trapped and adsorbed rubber in the vicinity of the filler. This suggests that, a decrease of adsorbed rubber content could be compensated by an increase of occluded and/or trapped rubbers contents, which leads to the same κ value

Then, κ defines more precisely than the specific surface area (derived from cDBPA) the effective surface in contact with rubber macromolecules. This surface is directly linked to the volume fraction of rubber with reduced mobility, which contributes to the reinforcement. However, this parameter does not quantify the reduction of mobility in this volume fraction. Then κ factor is consistent with both theories of onion like structure^{17,23} and gradient of mobility.^{16,29}

Indeed, the proportionality between κ and the effective filler volume fraction shows that κ takes account of the overall effective reinforcement. It is well related to the hydrodynamic effect in the linear viscoelastic range. In this investigation, the compensation was verified in the κ range between 18–50 $\text{m}^2 \text{g}^{-1}$. For $\kappa < 18 \text{ m}^2 \text{g}^{-1}$ means below cluster percolation threshold, the linear dependence of the parameter κ versus the effective filler fraction should be unchanged (Fig. 8 dotted line) at least until the volume fraction corresponding to the existence of the

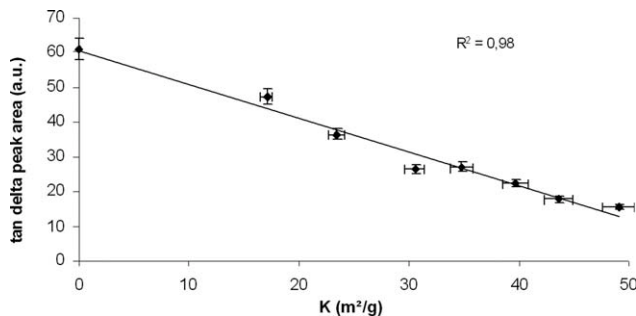


Figure 7 Influence of κ on the surface area under the peak principal relaxation of the matrix rubber.

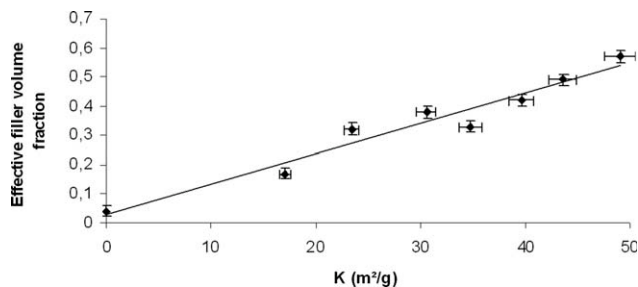


Figure 8 Influence of κ on effective filler volume fraction.

primary aggregates morphology as assumed by Mele et al.²⁵

CONCLUSION

During this work, we have analyzed the dynamic mechanical properties of carbon black filled synthetic elastomer. The tightly bound rubber content was modulated with the use of three carbon black grades incorporated at different loadings. Dynamic mechanical properties have shown an increase of $G'_{20^\circ\text{C}}$ and a decrease of both maximum $\tan \delta$ and $\tan \delta$ surface area peak with CB loading and/or increasing both structure and specific surface area. Those evolutions are attributed to the hydrodynamic interactions which can be measured by the effective filler volume fraction. In regard to the observations involving same evolution of dynamic mechanical properties versus CB loading and CB structure, a new parameter κ was defined in the linear behaviour. It takes into account the overall hydrodynamic effect of the effective filler volume fraction included occluded and tightly bound elastomer. Therefore, the relations between κ and both $G'_{20^\circ\text{C}}$ and $\tan \delta$ surface area peak gives good descriptions of the equivalence between CB loading and CB structure influence on hydrodynamic interactions involved in dynamic mechanical properties in the linear regime. It should be expected that the relevance of this parameter κ correspond to the range of CB loading from the isolated primary morphology aggregates in the rubber matrix until the persistence of this primary aggregates morphology unity in the clusters agglomerates. Further works to check this assumption are under way.

References

- Guth, E. *J Appl Physic* 1945, 16, 20.
- Medalia, A. I. *J Colloids Interface Sci* 1970, 32, 115.
- Medalia, A. I. *Rubber Chem Technol* 1973, 46, 877.
- Krauss, G. *Rubber Chem Technol* 1971, 44, 199.
- Gessler, A. M.; Hess, W. M.; Medalia, A. I. *Plast Rubber process* 1978, 3, 141.
- Roychoudhury, A.; De, P. P. *J Appl Polym Sci* 1995, 55, 9.
- Leblanc, J. L. *J Appl Polym Sci* 2000, 78, 1541.

8. Dutta, N. K.; Choudhury, N. R.; Haidar, B.; Vidal, A.; Donnet, J. B.; Delmotte, L.; Chezeau, J. M. *Rubber Chem Technol* 2001, 74, 260.
9. Choi, S. S. *J Appl Polym Sci* 2004, 93, 1001.
10. Berriot, J.; Montes, H.; Martin, F.; Mauger, M.; Pyckhout-Hintzen, W.; Meier, G.; Frielinghau, H. *Polymer* 2003, 44, 4909.
11. Legrand, A. P.; Lecomte, N.; Vidal, A.; Haidar, B.; Papirer, E. *J Appl Polym Sci* 1992, 46, 2223.
12. Lüchow, H.; Breier, E.; Gronski, W. *Rubber Chem Technol* 1997, 70, 747.
13. Vidal, A.; Haidar, B. *Die Angew Makromol Chem* 1992, 202, 133.
14. Sosson, F. Ph.D. Dissertation, Universite du Sud Toulon Var, France, 2007.
15. Kauffman, S.; Slichter, W. P.; Davie, D. D. *J Polym Sci Part A-2: Polym Chem* 1971, 9, 829.
16. Berriot, J.; Lequeux, F.; Monnerie, L.; Montes, H.; Long, D.; Sotta, P. *J Non Cryst Solids* 2002, 307, 719.
17. Leblanc, J. L. *Prog Polym Sci* 2002, 27, 627.
18. Dannenberg, E. M. *Rubber Chem Technol* 1986, 59, 512.
19. Medalia, A. I. *Rubber Chem Technol* 1978, 51, 437.
20. Choi, S. S. *J Polym Science Part B: Polym Phys* 2001, 39, 439.
21. Wang, M. J. *Rubber Chem Technol* 1998, 71, 520.
22. Fröhlich, J.; Niedermeier, W.; Luginsland, H. D. *Compos Part A* 2005, 36, 449.
23. Omnès, B.; Thuillier, S.; Pilvin, P.; Grohens, Y.; Gillet, S. *Compos Part A* 2008, 39, 1141.
24. Heinrich, G.; Kluppel, M. *Adv Polym Sci* 2002, 160, 1.
25. Mele, P.; Marceau, S.; Brown, D.; Puydt, Y.; Alberola, N. D. *Polymer* 2002, 43, 5577.
26. O'Brien, J.; Cashell, E.; Wardell, G. E.; McBrierty, V. J. *Macromolecules* 1976, 9, 653.
27. Choi, S. S.; Hwang, K. J.; Kim, B. T. *J Appl Polym Sci* 2005, 98, 2282.
28. Leblanc, J. L.; Stragliati, B. *J Appl Polym Sci* 1997, 63, 959.
29. Berriot, J.; Montes, H.; Lequeux, F.; Long, D.; Sotta, P. *Macromolecules* 2002, 35, 9756.
30. Johnson, M. A.; Beatty, M. F. *Int J Eng Sci* 1995, 33, 223.
31. Wang, M. J. Meeting of the Rubber Division; American Chemical Society: Indianapolis, Indiana, 1998; pp 1–34.